Journal of Materials Chemistry A

This article can be cited before page numbers have been issued, to do this please use: L. Chen, T. Yang, H. Cui, T. Cai, L. Zhang and C. Su, *J. Mater. Chem. A*, 2015, DOI: 10.1039/C5TA05592J.

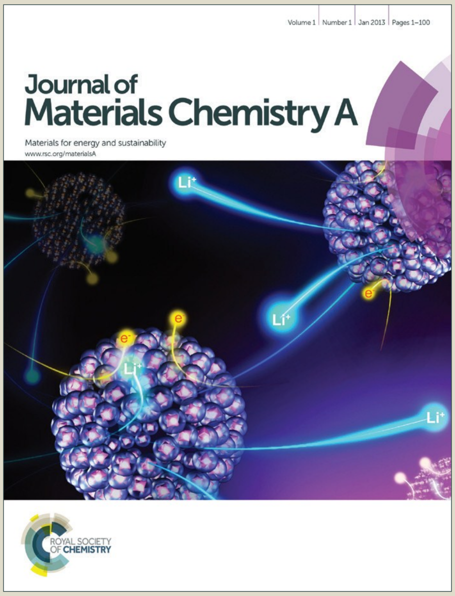

View Article Online
DOI: 10.1039/C5TA05592J

Journal Name

ARTICLE

A Porous Metal-Organic Cage Constructed from Dirhodium Paddle-Wheels: Synthesis, Structure and Catalysis

Received 00th January 20xx,
Accepted 00th January 20xx

DOI: 10.1039/x0xx00000x

www.rsc.org/

Lianfen Chen,[a] Tao Yang,[a] Hao Cui,[a] Tao Cai,[a] Li Zhang,*[,a] Cheng-Yong Su*[,a,b]

Self-assembly of dirhodium(II) tetraacetate ($Rh_2(OAc)_4$) with a dicarboxylic acid 3,3'-(1,3-phenylenebis(ethyne-2,1-diyl))dibenzoic acid (H_2pbeddb) gives rise to a metal-organic cage (MOC) containing Rh-Rh bonds with the formula of [Rh_4(pbeddb)$_4$(H_2O)$_2$(DMAC)$_2$] (MOC-Rh-**1**). Single-crystal X-ray diffraction analysis reveals that MOC-Rh-**1** shows a lantern-type cage structure, in which a pair of $Rh_2(CO_2)_4$ paddlewheels are linked by four diacid ligands. The dimensions of the inner cavity of MOC-Rh-**1** are 9.5×14.8 Å^2 (atom-to-atom distances across opposite metal and phenyl groups of pbeddb^{2-}). In the solid phase, the cages are aligned by π-π stacking to form one-dimensional channels (9.5 × 11.1 Å^2) through cage windows. Therefore, the crystalline samples of MOC-Rh-**1** are porous with the inner and outer cavities of the cages accessible in the heterogeneous condition. MOC-Rh-**1** has been fully characterized by EA, TGA, PXRD, IR, UV-vis and XPS measurements. The catalytic tests disclose that activated MOC-Rh-**1** is effective in the intramolecular C-H amination of vinyl, dienyl and biaryl azides, leading to the formation of indoles, pyrroles and carbazoles, respectively, and the porous catalyst can be recycled easily and used for at least nine runs without significant loss of activity. In the nine runs, the conversions were in the range of 93-99%, whereas in the tenth run, the conversion was reduced to 78%.

1. INTRODUCTION

Metal-organic cages (MOCs) have attracted significant research interests in the past two decades,[1] due to their applications in storage of reactive species,[2] drug delivery,[3] selective recognition or separation of species from a mixture,[4,5] catalysis,[6-10] etc. Most of the reported MOCs were constructed from single metal ions and neutral organic bridging ligands. The assembly of molecular architectures with metal clusters acting as nodes has not been widely explored. As a metal cluster node, the dinuclear paddle-wheel unit has emerged as a common four-connected building block in the synthesis of MOCs.[11-22] The introduction of metal-metal bonded clusters into molecular assemblies has not only expanded the field but also added electrochemical and spectroscopic probes to the study of such clusters.[11] Cotton and Murillo have employed dimetal units, especially Mo_2^{4+}, Rh_2^{4+} and Ru_2^{5+}, in the construction of polygons such as molecular loops, triangles and squares, as well as polyhedra such as tetrahedron and octahedron.[16-18] Yaghi and co-workers reported a variety of porous octahedra and cuboctahedra constructed from $Cu_2(CO_2)_4$ paddle-wheel building units.[19] Zhou et al. developed a series of MOCs derived from dimetal paddlewheel unis (Cu_2, Mo_2, and Ru_2 units) and dipotic carboxylate ligands with bridging angles of 0, 60, 90 and 120°.[20-22]

Recently, porous materials based on MOCs have been achieved and exhibited pre-designed pore properties.[1a] For example, the paddlewheel metal units used to form MOCs are widely employed in the syntheses of metal-organic frameworks (MOFs) with infinite channels. Through rational ligand design, novel porous MOF materials based on MOCs can be prepared.[23] Additionally, the crystal stacking of discrete MOCs in a proper packing mode, infinite channels through cage windows can be formed.[15b,21b] When these MOCs are used as solid materials, they can be considered porous materials, and therefore exhibit pore properties such as gas adsorption. More importantly, such heterogeneous MOC catalysts can promote both of the in-cage and out-cage reactions with high efficiency, considering that the active metal sites located in both of inner and outer surfaces can be accessed other than the polymer-supported catalysts with catalytically active sites on the exteriors alone.

Despite the availability of many MOCs containing dimetal units, only a limited number of them have been further applied in catalysis.[24] Whelan and coworker have utilized molecular loops $(Mo_2)_2L_2$ as catalysts for the polymerization of norbornene.[24a] Zhou et al.[24b] and us[24c] have prepared lantern-type polyhedral $(Cu_2)_2L_4$, which were then applied in cyclopropanation reactions. Dastidar et al. have reported a

---

[a] MOE Laboratory of Bioinorganic and Synthetic Chemistry, Lehn Institute of Functional Materials, School of Chemistry and Chemical Engineering, Sun Yat-sen University, Guangzhou 510275, China. E-mail: zhli99@mail.sysu.edu.cn; cesscy@mail.sysu.edu.cn

[b] State Key Laboratory of Organometallic Chemistry, Shanghai Institute of Organic Chemistry, Chinese Academy of Sciences, Shanghai 200032, China.

† Electronic Supplementary Information (ESI) available: Syntheses of ligand and azides, heterogeneous catalysis and recyclability, NMR spectra of pure products of indoles, pyrroles and carbazoles, TOF-MS spectra, single-crystal and powder X-ray diffraction (PXRD) analyses, XPS spectra. CIF files giving crystallographic data. See DOI: 10.1039/x0xx00000x

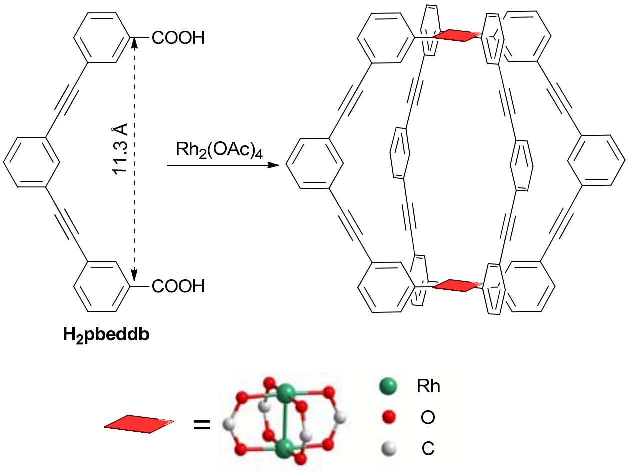

Scheme 1. MOC Synthesis.

truncated octahedron $(Cu_2)_6L_8$ and examined its catalytic activity in the oxidation of benzyl alcohol to benzaldehyde.[24d] Cotton and Murillo have developed molecular triangles $(Rh_2)_3L_3$ and used them in asymmetric cyclopropanation.[24]

Meanwhile, dirhodium complexes are commonly used catalyst due to their diverse catalytic reactivity, especially in nitrene transfer reactions.[25] The activation of C-H bonds by dirhodium(II) nitrenoids allows access to valuable carbocycles and hetereocycles efficiently. Since azides are readily available and the only byproduct is N_2, the prospect of rhodium nitrenoid generation from them is highly appealing. Driver recently discovered that rhodium(II) carboxylates can catalyze the intramolecular formation of C-N bonds from vinyl, dienyl and biaryl azides to provide indoles, pyrroles and carbazoles, respectively.[26]

To the best of our knowledge, there were two reports of MOCs based on dirhodium(II) paddlewheel units, but none of them have been tested in nitrene transfer reactions.[17b,c] In this work, a lantern-type MOC of $[Rh_4(pbeddb)_4(H_2O)_2(DMAC)_2]$ (MOC-Rh-**1**) (pbeddb^{2-} = 3,3'-(1,3-phenylenebis(ethyne-2,1-diyl))dibenzoate)) has been synthesized from the self-assembly of $Rh_2(OAc)_4$ and the rigid diacid H$_2$pbeddb (Scheme 1), which was then employed in C-H amination reactions with azides.

2. EXPERIMENTAL SECTION

2.1 General

All the reagents in the present work were obtained from the commercial source and used directly without further purification. The ligand 3,3'-[1,3-phenylenebis(ethyne-2,1-diyl)]dibenzoic acid (H$_2$pbeddb) was synthesized according to the literature.[21b] Vinyl azides, dienyl azides and biaryl azides are prepared following the reported precedures.[27] The elemental analyses were performed with Perkin-Elmer 240 elemental analyzer. HRESI-MS was performed by using a Bruker Daltonics ESI-Q-TOF maXis4G. The data analyses of ESI-TOF mass spectra were processed on Bruker Data Analysis software and the simulations were performed on Bruker Isotope Pattern software. Infrared spectra on KBr pellets were collected with a Nicolet/Nexus-670 FT-IR spectrometer in the region of 4000-400 cm^{-1}. UV-vis spectra were tested on a Shimadzu/UV-3600 spectrophotometer. ^{1}H NMR spectra were recorded on Varian/Mercury-Plus 300MHz or on Bruker AVANCE III 400MHz. Chemical shifts were quoted in parts per million (ppm) referenced to the appropriate solvent peak or 0 ppm for TMS. PXRD patterns were recorded on SmartLab X-ray powder diffractometer (Rigaku Co.) at 40 kV and 30 mA with a Cu target tube. Thermogravimetric (TG) analyses were performed under an N_2 atmosphere at a heating rate of 10 °C min^{-1} by using a NETZSCH TG 209 system. X-ray photoelectron spectroscopy (XPS) was performed on a ULVAC PHI Quantera microprobe. Binding energies (BE) were calibrated by setting the measured BE of C 1s to 284.65 eV. ICP spectroscopy was conducted on a Spectro Ciros Vision ICP-OES spectrometer that is equipped with vacuum optics covering the spectral range from 175-777 nm, plasma power, 1300 w; coolant flow, 15.00 L/min; auxiliary flow, 0.80 L/min; nebulizer 0.70 L/min. The sorption isotherms for N_2 (77 K) and CO_2 (195 K) gas were measured with an Autosorb-iQ2-MP gas sorption analyzer (Quantachrome, USA). The samples are vacuumed at 110 °C for 6 h before the sorption examination.

Cautions! Although we have not experienced any problem in the handling of the azides (e.g. vinyl azides, dienyl azides and biaryl azides), extreme care should be taken when manipulating them due to their explosive nature.

2.2 Synthesis of $[Rh_4(pbeddb)_4(H_2O)_2(DMAC)_2]$ (MOC-Rh-1)

H$_2$pbeddb (18.3 mg, 0.05 mmol), $Rh_2(OAc)_4$ (8.8 mg, 0.02 mmol), Na_2CO_3 (6.0 mg 0.057 mmol) and dimethylacetamide (DMAC, 4 mL) were placed in a glass vial, which was then sealed and heated to 100 °C in an oven. After 24 h, green block crystals were obtained (11.2 mg, 54% yield based on $Rh_2(OAc)_4$). Anal. Calcd. for $C_{124}H_{127}N_7O_{31}Rh_4$ (MOC-Rh-**1**·6H$_2$O·5DMAC): C, 56.78; H, 4.88, N, 3.74%; Found: C, 56.55; H, 4.98; N, 3.85%. FTIR (KBr) *v* 3431 (s, br), 2919 (w), 1625 (m), 1606 (w), 1462 (w), 1425(w), 1387 (m), 1343 (w), 1082 (m. br), 784 (w) cm^{-1}.

2.3 X-ray Crystallography

The X-ray diffraction data were collected with an Agilent Technologies SuperNova X-RAY diffractometer system for MOC-Rh-**1** equipped with Cu$_{k\alpha}$ radiation (λ = 1.54178 Å). The crystal was kept at 150.00(10) K during data collection. Using Olex2[28], the structure was solved with the ShelXS-97[29] structure solution program using Direct Methods and refined with the XL[30] refinement package using Least Squares minimization. The positions of the hydrogen atoms were generated geometrically. A summary of the crystal structure refinement data and selected bond angles and distances are listed in Table 1 and Table S1. Crystallographic data for the structure have been deposited in the Cambridge Crystallographic Data Center with CCDC reference number 1057865.

2.4 Typical Procedure for the Catalytic C-H Bond Amination Reactions

Toluene (0.75 mL) was added to the mixture of (*Z*)-methyl 2-azido-3-phenylacrylate (**2a**, 30.4 mg, 0.15 mmol) and activated

View Article Online
DOI: 10.1039/C5TA05592J

Table 1. Crystal data and structure refinement parameters

	MOC-Rh-**1**·$2H_2O$·3DMAC
Formula	$C_{121}H_{110}N_7O_{28}Rh_4$
Fw	2521.80
T/K	150
Crystal system	triclinic
Space group	*P*-1
a/Å	14.3649(9)
b/Å	15.5751(10)
c/Å	16.3871(12)
α/°	72.966(7)
β/°	73.450(6)
γ/°	68.665(6)
Volume/$Å^3$	3199.2(4)
Z	1
$\rho_{calc}g/cm^3$	1.309
μ/mm^{-1}	4.685
F(000)	1289.0
Total/Unique	20800 / 10596
R_{int}	0.0417
Goodness-of-fit on F^2	1.036
R1, *wR*2 [I>=2σ (I)]	0.0591, 0.1697
R1, *wR*2 [all data]	0.0905, 0.1986

MOC-Rh-**1** (6.0 mg, 0.003 mmol, 2 mol%), then the whole suspension was heated to 60 °C for 16h before cooled to room temperature. The catalyst was removed through centrifugation, and washed with ethyl acetate (5 mL × 2). The combined supernatant was evaporated to dryness. The conversion of the reaction was monitored by ^{1}H NMR (400 MHz) spectroscopy. After that, the reaction mixture was separated by flash chromatography (1:20 EtOAc: hexanes) to obtain pure product methyl 1*H*-indole-2-carboxylate (**3a**) as white solid (24.7 mg, 94%).

2.5 Procedure for Recycling Study

A mixture of **2a** (101.5 mg, 0.50 mmol) and activated MOC-Rh-**1** (40.0 mg, 4 mol%) in toluene (2.5 mL) was heated at 85 °C for 8 h. The catalyst was separated by centrifugation, washed with ethyl acetate (5 mL × 3), dried under vacuum at 110 °C for 6 h and reused in the consecutive run. The conversion of the reaction was monitored by ^{1}H NMR spectroscopy.

2.6 ICP Spectrometric Evaluation

A mixture of **2a** (60.9 mg, 0.30 mmol) and activated MOC-Rh-**1** (12.0 mg, 2 mol%; containing *ca* 2.460 mg of Rh) in toluene (1.5 mL) was heated at 60 °C for 16 h. After cooled to room temperature, the reaction mixture was passed through a sand core funnel (G5) with a pad of celite, and washed with ethyl acetate (5 mL × 3). The combined solvent was treated with nitric acid (2 mL) and hydrochloric acid (6 mL) after concentrated to about 0.5 mL. The whole mixture was allowed to stay at room temperature for 3 h and heated at 150 °C to reduce the total volume to about 0.5 mL. Afterward, the reaction mixture was added with nitric acid (6 mL) and aqueous hydrogen dioxide (30 wt%, 1 mL), stayed at room temperature for 3 h, and then concentrated to 0.5 mL. The digestion procedure was repeated twice. The resulted colourless solution was diluted volumetrically with an aqueous solution of nitric acid (2%) to 10 mL, which was then evaluated by inductively coupled plasma optical emission spectrometer (ICP-OES) for Rh contents. The Rh contents were measured in ppm based on calibration curves obtained with a series of calibration standard solutions doped with different amount of Rh. The measured Rh content was 2.037 ppm (0.02037 mg), and the leached Rh% should be 0.8%, using the calculation equation "100% × (0.02037 mg / 2.460 mg)".

2.7 Hot Filtration Experiment

Two parallel C-H amination reactions of **2a** (60.0 mg, 0.30 mmol) in the presence of 2 mol% of activated MOC-Rh-**1** (12.0 mg) were heated in toluene (1.5 mL) at 60 °C. After 6 h, a group of reaction mixture was filtrated with filtration membrane (0.45 μm), and the filtrate was allowed to stand at 60 °C for another 10 h. The other group of reaction mixture stayed with catalyst for further reaction without any treatment. The conversions of the reactions were monitored by ^{1}H NMR.

3. RESULTS AND DISCUSSION

3.1 Design of MOC Catalysts with Rh-Rh Bonds

Tetracarboxylate Rh dimers, while are stable to many conditions, including strong acid, participate freely in ligand exchange reactions. It was hypothesized that carboxylate detachment from the dinuclear Rh core was responsible for catalyst degradation. To prevent the ligands from dissociating from the metal centers, bridged dirhodium complexes, which were based on bridging diacid ligands, have been developed.[31] The well-designed bridged dirhodium carboxylates have been widely used in carbene and nitrene transfer reactions, exhibiting superior performances in terms of turnover number and reaction efficiency. We are interested in an alternative strategy for improving the kinetic stability of dirhodium(II) complexes through connecting two and more dimetal untis (Rh_2^{4+}) with dicarboxylates to form higher order structures such as polyhedra.[17b] Taking account of more interactions existing in these polyhedra, we hypothesize that they were less prone to ligand exchange than other simple tetracarboxylate systems (e.g. $Rh_2(OAc)_4$) derived from monocarboxylic acids. The ligand 3,3'-[1,3-phenylenebis(ethyne-2,1-diyl)]dibenzoic acid (H_2pbeddb) was chosen for our MOC catalyst design. As shown in Scheme 1, the anion pbeddb^{2-} has a bridging angle of 0° and a long bridging spacer spanning 11.3 Å, and is useful for the construction of large porous MOCs. Zhou et. al. and Lah et al. have previously prepared MOCs, derived from dimetal paddlewheel units (Mo_2 and Cu_2 units) and H_2pbeddb.[15b,21b]

The crystal structures of the lantern-type MOCs of $Mo_4(pbeddb)_4(S)_x$ (S represents for solvents) and $Cu_4(pbeddb)_4(S)_x$ possess internal cavities of 9.7 × 15.4 and

View Article Online
DOI: 10.1039/C5TA05592J

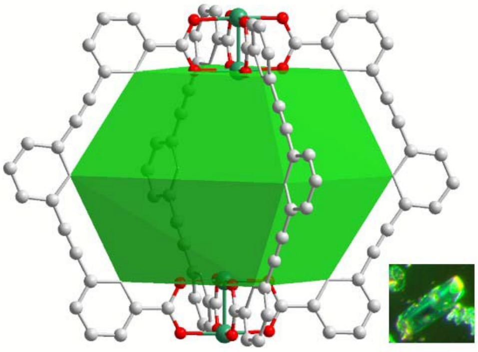

Figure 1. Ball and stick diagram of MOC-Rh-**1**. The insert picture is the photograph of the single crystals. The bright green polygon only serves to guide visualization, not to represent the actual size of the cavity. Rh (Sea green), O (red), C (gray). All hydrogen atoms and solvent molecules including those coordinated to Rh-Rh units are omitted for clarity.

9.0 × 14.8 Å^2 (atom-to-atom distances across opposite metal and phenyl groups of pbeddb^{2-}), respectively. The crystal packing patterns of these MOCs are also interesting. Both of $Mo_4(pbeddb)_4$ and $Cu_4(pbeddb)_4$ are crystallized in *P*-1, and the inter-cage π-π stacking interactions lead to infinite channels with the dimensions of 9.7 × 10.7 and 9.0 × 11.1 Å^2, respectively. The structure rationale of the above MOCs assembled from pbeddb^{2-} and dimetal units suggested that the metal centers located in both of inner and outer surfaces were accessible to the substrates, which might highly increase the reaction efficiency. We herein desire to develop MOCs with Rh-Rh bonds derived from H_2pbeddb, which have not been reported previously.

3.2 Synthesis and Crystal Structure

The reaction of H_2pbeddb with $Rh_2(OAc)_4$ in dimethylacetamide (DMAC) in the presence of Na_2CO_3 gave rise to green block crystals of $[Rh_4(pbeddb)_4(H_2O)_2(DMAC)_2]\cdot 2H_2O\cdot 3DMAC$ (MOC-Rh-**1**·$2H_2O\cdot 3$DMAC) (Figure 1). Single-crystal X-ray diffraction analysis revealed that it crystallizes in the triclinic centro symmetric space group *P*-1. MOC-Rh-**1** is composed of discrete lantern-type cages, and each cage contains four dicarboxylic ligands and two $Rh_2(COO)_4$ paddle-wheel moieties. Each paddle-wheel moiety is further coordinated with two molecules in the axial positions, either of H_2O for the inner Rh(II) atom or DMAC for the exterior Rh(II) atom. As a result, the axial coordinated solvents might be removed, leaving both the inner and the outer Rh(II) metal sites for catalysis. The Rh-Rh distance in each dirhodium moieties is 2.39 Å, which is in accordance with the reported values for the Rh–Rh bond length in Rh-carboxylate complexes, and this bond length is generally in the range of 2.34-2.41 Å.[11] The dimensions of the cage excluding coordinated solvents are approximately 1.4 nm in height (Rh¨Rh) and 2.0 nm in diameter (Ph¨Ph between two opposite ligands). The window of the cage formed by two pbeddb^{2-} ligands is about 9.6 Å high, 11.1 Å wide for the larger ones and 10.0 Å for the smaller ones (Figure S1). The dimensions of the inner cavity of the MOC are 9.5 × 14.8 Å^2 (atom-to-atom distances across opposite metal and phenyl groups of pbeddb^{2-}).

Three different types of inter-cage π-π stacking interactions between the phenyl groups of the ligands have been observed (Figure S2 and Table S2). The interactions lead to honeycomb shape solvent-filled channels (9.5 × 11.1 Å^2) with an overall 49.4% solvent-accessible volume calculated using the PLATON[32] (Figure 2). One interesting feature of these channels is that they pass through the windows of the discrete cages. As a result, both of inner-cage and outer-cage metal sites of the dirhodium metal units in its desolvated form can be accessible to the incoming guests.

Control experiments revealed that the alkali Na_2CO_3 was essential for the syntheses of crystals suitable for single-crystal X-ray diffraction. Excess (larger than 1.5 eq. relative to the ligand H_2pbeddb) caused precipitation, however. We also found that the solvents play an important role. When a mixed solvent of dimethylformamide (DMF) and H_2O (v/v=4/1) was used instead of DMAC, purple crystals were obtained. Single crystal structure analysis disclosed that the structure was almost the same with MOC-Rh-**1** except for the solvents coordinated to the outer Rh(II) atoms. Unfortunately, we can not determine the axial solvents based on its single X-ray crystal data. We speculate that they were nitrogen-containing

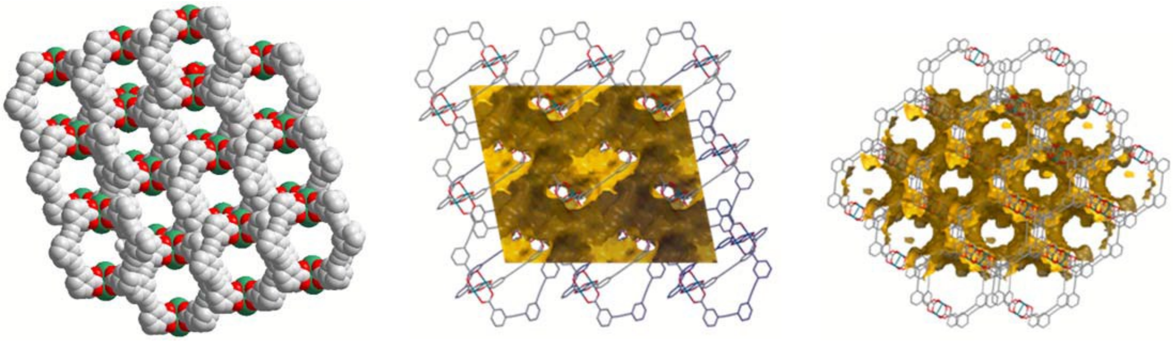

Figure 2. Solid-packing of MOC-Rh-**1** in the crystal lattice. Left: 1D channels formed through cage windows; Middle and right: the accessible voids viewed from different directions. Solvent molecules are omitted for clarity. Rh (sea green), O (red), C (gray).

View Article Online
DOI: 10.1039/C5TA05592J

molecules, which might come from the decomposition of DMF. On the basis of the study of Johnson et al. and Jessop et al. on the coordination effects of solvents, dirhodium(II) complexes with oxygen-containing solvents (e.g. H_2O, THF) in the axial position were usually in green, whereas those with nitrogen-containing solvents (e.g. DMF, MeCN, NEt_3) were often in purple.[33]

3.3 Physical Characterizations

To investigate the phase purity of bulk sample, MOC-Rh-**1** was subjected to powder X-ray diffraction (PXRD) test. In air, the crystals are apt to effloresce probably due to the escape of lattice solvents. When measured in a sealed capillary tube with the solvent, the PXRD patterns show comparable diffraction profile with the simulated one based on the single crystal (Figure S3), while some peaks are slightly shifted probably owing to the exchange of solvent molecules.

Thermogravimetric analysis (TGA) of the as-synthesized MOC-Rh-**1** sample showed a total weight loss of 28.6% in the range of 30-210 °C, corresponding to the escape of lattice and coordinated solvent molecules (expected 28.7%, Figure 3). Above 350 °C, an abrupt weight loss appears, indicative of the decomposition of the cages. To examine whether the solvents could be removed prior to further applications such as gas adsorption and catalysis, the as-synthesized sample of MOC-Rh-**1** has been activated by heating at 110 °C under vacuum for 6 h. As shown in the TG curve of activated MOC-Rh-**1**, only 6.3% of weight loss occurred below 350 °C, suggesting that most of the solvents have been removed.

The infrared spectrum of MOC-Rh-**1** is similar to that of reported dirhodium(II) tetracarboxylates.[33a] The asymmetric stretching vibrations (ν_{as}(COO)) and symmetric stretching vibrations (ν_s(COO)) of the coordinate carboxylate groups are observed at 1625 and 1462 cm^{-1}, respectively. The splitting Δ value of 163 between these two bands (ΔCOO= ν_{as} (COO) - ν_s (COO)) might indicate the carboxylate groups in bridging bidentade coordination mode,[34] which is in consistent with the single-crystal X-ray diffraction analyses.

The solid UV-vis spectrum of the as-synthesized MOC-Rh-**1** sample was shown in Figure 4, which displayed two principal bands at 453 and 587 nm. These two bands are characteristic of the dirhodium paddle-wheel structure, which is absent in the absorption spectrum of the organic ligand. The assignment of the higher energy band (453 nm) is uncertain, although it has been attributed to a π^*(Rh-O)$\rightarrow\sigma^*$(Rh-O) transition.[35] The lower energy band is assigned to the HOMO-LUMO ($\pi^*(Rh_2)\rightarrow\sigma^*(Rh_2)$) transition, which is strongly affected by the axial solvents.[36] The λ_{max} for the lower energy peak shifts to longer wavelengths by only 8 nm (Table S3) after the as-synthesized sample was activated under vacuum at 110 °C for 6 h. On the basis of the data, we speculated that most of the coordinated solvents remained on the metal sites under our activation process. Nevertheless, activated MOC-Rh-**1** could be used for catalysis, considering that the coming substrates could replace these coordinated solvents due to larger affinity between the former and the Rh(II) metal sites.

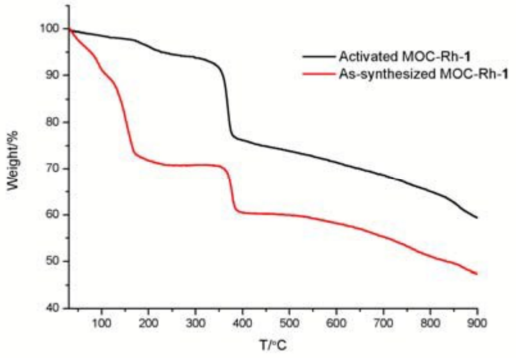

Figure 3. The TG curves of as-synthesized and activated MOC-Rh-**1**.

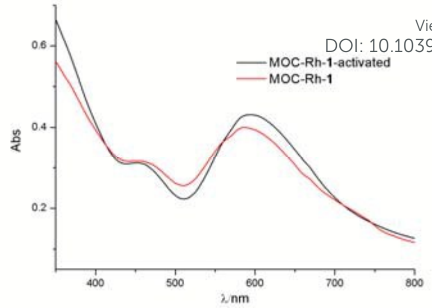

Figure 4. Solid UV-vis spectra of as-synthesized and activated sample of MOC-Rh-**1**.

To evaluate the porosity and storage capability of MOC-Rh-**1**, the adsorption isotherms of N_2 at 77 K as well as CO_2 at 195 K have been studied (Figure 5). Before the measurements, the bulk samples of MOC-Rh-**1** were activated through heating at 110 °C under vacuum for 6 h. The N_2 sorption isotherm of activated MOC-Rh-**1** at 77K does not show any appreciable amount of adsorption. However, at 195 K and 1 atm, the uptake of CO_2 is 33.9 cm^2g^{-1}, corresponding to about 3 CO_2 molecules adsorbed per MOC-Rh-**1** molecule. Based on the CO_2 adsorption isotherm a 195 K, the BET surface area of MOC-Rh-**1** is calculated to be about 95 m^2g^{-1}. The selective gas adsorption for CO_2 over N_2 have been observed in other lantern-type MOCs such as activated $Cu_4(pbeddb)_4(S)_x$ and $Cu_4(nddb)_4(S)_x$ (H_2nddb = 3,3'-(naphthalene-2,7-diyl)dibenzoic acid).[15b,23b]

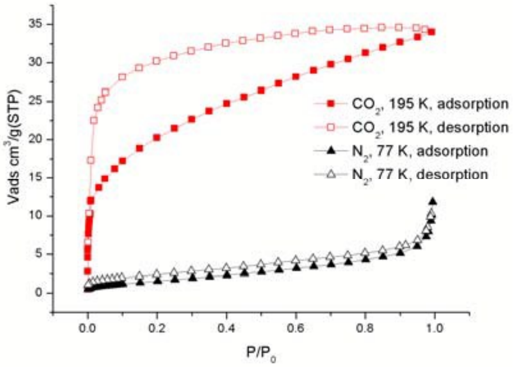

Figure 5. Gas adsorption/desorption isotherms of N_2 (77K) and CO_2 (195K) of activated MOC-Rh-**1**. Solid symbols, adsorption; open symbols, desorption.

View Article Online
DOI: 10.1039/C5TA05592J

3.4 Catalytic Performances

C-H amination in the homogeneous phase has been greatly enhanced due to improved methods of the synthesis of rhodium nitrene intermediates.[25] MOC-Rh-**1** isn't dissolved in common organic solvents, such as toluene, DMSO, DMF, H_2O, acetone and acetonitrile, which indicates that it might act as a heterogeneous catalyst. It is noted that MOC-Rh-**1** possesses large inner and outer cavities, whose sizes are 9.5×14.8 Å^2 and 9.5×11.1 Å^2, respectively, suggesting that the catalytic reactions might occur both on the internal and external surfaces of the crystal catalysts.

The evaluation of the heterogeneous catalytic capabilities of activated MOC-Rh-**1** was carried out using C-H amination of vinyl azides. The homogeneous protocol has been successfully elaborated by Driver et al. and has transformed vinyl azides (e.g. (*Z*)-methyl 2-azido-3-arylacrylate) into indoles in high yields, using rhodium(II) perfluorobutyrate ($Rh_2(O_2CC_3F_7)_4$) as the catalyst.[26a] As can be seen in Table 2, the reaction of (*Z*)-methyl 2-azido-3-phenylacrylate (**2a**) as well as (*Z*)-methyl 2-azido-3-(4-methoxyphenyl)acrylate (**2b**) in the presence of 2 mol% of activated MOC-Rh-**1** was accomplished with larger than 99% conversion after 16 h at 60 °C, leading to the formation of the indoles **3a** and **3b** in 94% and 91% yield, respectively (entries 1 and 2). By contrast, the yields for (*Z*)-methyl 2-azido-3-(*p*-tolyl)acrylate (**2c**) and (*Z*)-methyl 2-azido-3-(1,1'-biphenyl)acrylate (**2d**) were reduced to 64% and 44%, respectively, under the same reaction conditions at 60 °C (entries 3 and 4). Increasing the reaction temperature to 85 °C could significantly improve the yields with up to 90% for **3c** and 62% for **3d** in 3 h and 24 h, respectively. Halogen substituted azides **2e-g** showed much poorer performances, and the corresponding indoles **3e-g** were obtained in less than 60% yields when the catalytic reactions were heated at 60 °C for 16 h (entries 5-7). Similarly, **3e-g** can be prepared in much higher yields at a higher temperature, and the isolated yields were 92%, 86% and 78%, respectively, at 85 °C in 5 h. In addition to indoles, aromatic *N*-heterocycles such as **3h** can be accessed from 1-substituted naphthalene vinyl azide (entry 8). Driver et al. have also showed that pyrroles and carbazoles could be produced from the similar intramolecular C-H amination of dienyl azides and biaryl azides, respectively.[26b,d] On the basis of their homogeneous protocols, we further tested the catalytic capability of activated MOC-Rh-**1** in the syntheses of pyrroles and carbazoles. Methyl 5-phenyl-1*H*-pyrrole-2-carboxylate (**4**) and 9*H*-carbazole (**5**) can be obtained in high yields under optimized reaction conditions in the presence of activated MOC-Rh-**1** (entries 9 and 10). We have also tested the catalytic activity of the $Cu_4(pbeddb)_4$, $Rh_2(OAc)_4$ and $RhCl_3$ in the C-H intramolecular amination of **2a** (Table S4). No reaction occurs in the presence of $Cu_4(pbeddb)_4$ or $RhCl_3$. The conversion in the presence of $Rh_2(OAc)_4$ is 11%. Our MOC catalyst, MOC-Rh-**1**, shows obvious advantages over them.

Table 2. Substrate Scope of Catalytic C-H Amination[a]

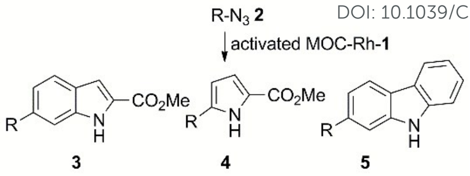

entry	product	entry	product
1	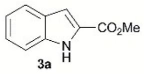 3a 94%	2	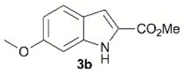 3b 91%
3	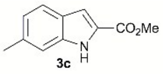 3c 64% (90%[b])	4	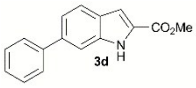 3d 44% (62%[c])
5	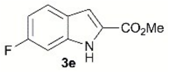 3e 54% (92%[d])	6	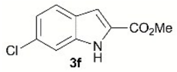 3f 32% (86%[d])
7	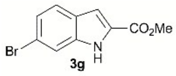 3g 28% (78%[d])	8	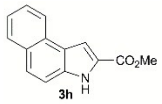 3h 88%
9	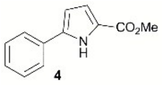 4 98%[e]	10	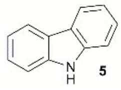 5 92%[f]

[a]Reaction conditions: 2 mol% of the catalyst, 60 °C, 16 h, toluene. The yields are isolated yields. [b]85 °C, 3 h. [c]85 °C, 24 h. [d]85 °C, 5 h. [e]0.5 mol% of the catalyst load, 85 °C, 2 h. [f]3 mol% of the catalyst load, DME, 85 °C, 16 h.

In $Rh_2(O_2CC_3F_7)_4$-catalyzed intramolecular C-H amination of azides, it is proposed that the reaction proceeds through the rhodium nitrenoid intermediate, the electronic donation by the 4-substituted group (e.g. 4-OMe) accelerates the formation of rhodium nitrenoid and the C-N bond formation occurs through a 4π-electron-5-atom electrocyclization.[26l] In this mechanism, 3-methoxy group in (*Z*)-methyl 2-azido-3-(3-methoxyphenyl)acrylate (**2i**) acts as an inductive electron-withdrawing group and slows down the formation of rhodium nitrenoid. We have examined the reaction of 3-methoxy substituted azide **2i** in the presence of 2 mol% MOC-Rh-**1** and heating at 60 °C for 16 h. The reaction was very messy, and a 1:1 mixture of 5- and 7-regioisomers was obtained in less than 30% yield. The data indicate that the MOC-Rh-**1** catalyzed C-N bond formation reaction occurs through a similar 4π-electron-5-atom electrocyclization as the Driver's protocol.

To verify the reactions were heterogeneous but not catalyzed by dissociated Rh species that were leached into the reaction solutions, we carried out a hot filtration experiment (Figure 6). At the 26% conversion of intramolecular the C-H amination reaction of **2a** in the presence of activated MOC-Rh-**1** for 6 h, the reaction mixture was filtrated with filtration membrane (0.45 μm), and the filtrate was allowed to stand for another 10 h. The conversion of the supernatant rose to 36%

View Article Online
DOI: 10.1039/C5TA05592J

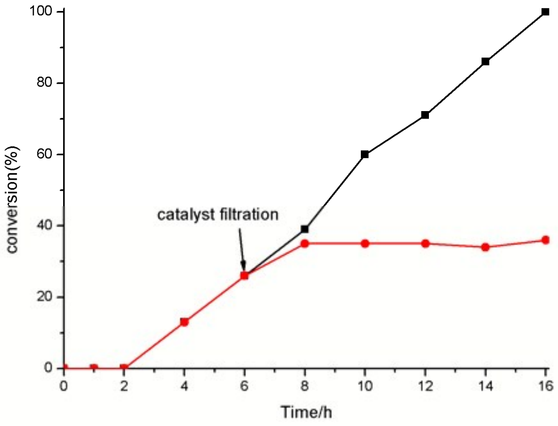

Figure 6. Filtration experiment for activated MOC-Rh-**1**. Conversions are given as a function of time. The full square (■) represents the reaction with MOC-Rh-**1** as a catalyst. The full cycle (●) represents the reaction after removal of catalyst MOC-Rh-**1** at (26%) conversion.

with 10% increase. In contrast, control experiments show that a parallel reaction with the catalyst reached around 100% conversion after the same reaction time. Based on the filtration experiment, we believe that the reaction is basically heterogeneous, and we ascribe the additional 10% conversion to the leached Rh during the reaction. Inductively coupled plasma optical emission spectrometer analysis of the reaction filtrate indicated that the amount of the rhodium leaching into the reaction mixture was 0.8% of the total Rh content in MOC-Rh-**1**.

One remarkable feature of this C-H amination catalysis is that the MOC catalyst can be easily isolated by centrifugation and can be reused at least nine times without significant loss of activity (Figure 7, Table S4). In the nine runs, the conversions of **2a** were in the range of 93-99%, whereas in the tenth run, the conversion was reduced to 78%. To verify the valence states of the Rh in the recycled catalyst, X-ray photoelectron spectroscopy (XPS) has been carried out. As shown in Figure S4, the XPS spectrum displayed two intense peaks at 313.9 and 309.2 eV assigned to Rh $3d_{3/2}$ and Rh $3d_{5/2}$, indicative of the +2 valence nature of Rh. According to the literatures, the $3d_{5/2}$ binding energy of oxidized Rh^{2+} is in the range of 308.4 and 309.3 eV.[37]

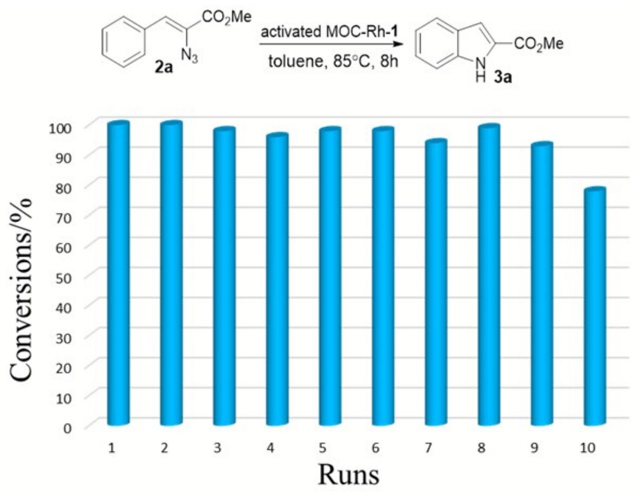

Figure 7. Recycling experiments.

4. CONCLUSION

A reproducible synthesis of a lantern-type metal-organic cage (MOC-Rh-**1**) consisting of two dirhodium units joined by four ditopic dicarboxylic ligands has been established. The well-designed MOC catalyst possesses more active Rh(II) sites than the general polymer-supported heterogeneous Rh(II) complexes with the active metal sites on the external surfaces alone. Depending on the crystal structures, the MOC possesses large windows (9.6 × 11.1 $Å^2$), and provide a platform to carry out reactions in its cavities. Additionally, the large channels (9.5 × 11.1 $Å^2$) formed by the crystal stacking of discrete MOCs make it possible that the catalytic reactions occur within the channels. Catalytic tests show that it can efficiently promote the intramolecular C-H amination of azides, and the catalyst can be recycled easily and used for at least nine runs without significant loss of activity. These catalytic results are quite encouraging and we are currently pursuing the design and synthesis of more MOC catalysts with Rh-Rh bonds.

ACKNOWLEDGMENT

This work was supported by the 973 Program (2012CB821701) and the NSFC Projects (21373278, 21102186, 91222201, 21173272, 21450110063), the NSF of Guangdong Province (S2013030013474) and the RFDP of Higher Education of China (20120171130006).

Notes and references

1 (a) T. R. Cook, Y.-R. Zheng and P. J. Stang, *Chem. Rev.*, 2013, **113**, 734-777. (b) M. M. J. Smulders, I. A. Riddell, C. Browne and J. R. Nitschke, *Chem. Soc. Rev.*, 2013, **42**, 1728-1754. (c) H. Amouri, C. Desmarets and J. Moussa, *Chem. Rev.*, 2012, **112**, 2015-2041. (d) M. Yoshizawa, J. K. Klosterman and M. Fujita, *Angew. Chem., Int. Ed.*, 2009, **48**, 3418-3438. (e) C. G. Oliveri, P. A. Ulmann, M. J. Wiester and C. A. Mirkin, *Acc. Chem. Res.*, 2008, **41**, 1618-1629. (f) D. Fiedler, D. H. Leung, R. G. Bergman and K. N. Raymond, *Acc. Chem. Res.*, 2005, **38**, 351-360. (g) J. Liu, L. Chen, H. Cui, J. Zhang, L. Zhang and C.-Y. Su, *Chem. Soc. Rev.*, 2014, **43**, 6011-6061.

2 (a) J. W. Leeland, F. J. White and J. B. Love, *J. Am. Chem. Soc.*, 2011, **133**, 7320-7323. (b) P. Mal, B. Breiner, K. Rissanen and J. R. Nitschke, *Science*, 2009, **324**, 1697-1699. (c) K. Li, L. Y. Zhang, C. Yan, S. C. Wei, M. Pan, L. Zhang and C. Y. Su, *J. Am. Chem. Soc.*, 2014, **136,** 4456-4459.

3 J. E. M. Lewis, E. L. Gavey, S. A. Cameron and J. D. Crowley, *Chem. Sci.,* 2012, **3**, 778-784.

4 (a) S. Tashiro and M. Fujita, *Bull. Chem. Soc. Jpn.,* 2006, **79**, 833-837. (b) Y. R. Hristova, M. M. J. Smulders, J. K. Clegg, B. Breiner and J. R. Nitschke, *Chem. Sci.*, 2011, **2**, 638-641. (c) S. Turega, M. Whitehead, B. R. Hall, M. F. Haddow, C. A. Hunter and M. D. Ward, *Chem. Commun.,* 2012, **48**, 2752-2754.

5 (a) T. F. Liu, Y. Liu, W. M. Xuan and Y. Cui, *Angew. Chem., Int. Ed.,* 2010, **49**, 4121-4124. (b) W. M. Xuan, M. N. Zhang, Y. Liu,

View Article Online
DOI: 10.1039/C5TA05592J

Z. J. Chen and Y. Cui, *J. Am. Chem. Soc.*, 2012, **134**, 6904-6907. (c) J. Dong, Y. Zhou, F. Zhang and Y. Cui, *Chem. Eur. J.,* 2014, **20**, 6455-6461.

6 (a) M. Yoshizawa, T. Kusukawa, M. Fujita and K. Yamaguchi, *J. Am. Chem. Soc.*, 2000, **122**, 6311-6312. (b) M. Yoshizawa, S. Miyagi, M. Kawano, K. Ishiguro and M. Fujita, *J. Am. Chem. Soc.,* 2004, **126**, 9172-9173. (c) Y. Nishioka, T. Yamaguchi, M. Kawano and M. Fujita, *J. Am. Chem. Soc.,* 2008, **130**, 8160-8161.

7 (a) M. D. Pluth, R. G. Bergman and K. N. Raymond, *Angew. Chem., Int. Ed.*, 2007, **46**, 8587-8589. (b) M. D. Pluth, R. G. Bergman and K. N. Raymond, *Science,* 2007, **316**, 85-88. (c) C. J. Brown, R. G. Bergman and K. N. Raymond, *J. Am. Chem. Soc*., 2009, **131**, 17530-17531. (d) C. J. Hastings, M. D. Pluth, R. G. Bergman and K. N. Raymond, *J. Am. Chem. Soc.,* 2010, **132**, 6938-6940. (e) C. J. Brown, G. M. Miller, M. W. Johnson, R. G. Bergman and K. N. Raymond, *J. Am. Chem. Soc.,* 2011, **133**, 11964-11966. (f) C. Zhao, Q. F. Sun, W. M. Hart-Cooper, A. G. Dipasquale, F. D. Toste, R. G. Bergman and K. N. Raymond, *J. Am. Chem. Soc*., 2013, **135**, 18802-18805.

8 (a) D. H. Wang, B. G. Zhang, C. He, P. Y. Wu and C. Y. Duan, *Chem. Commun.,* 2010, **46**, 4728-4730. (b) X. Wu, Z. H. Lin, C. He and C. Y. Duan, *New. J. Chem.,* 2012, **36**, 161-167. (c) Y. Jiao, J. Wang, P. Y. Wu, L. Zhao, C. He, J. Zhang and C. Y. Duan, *Chem. Eur. J.*, 2014, **20**, 2224-2231. (d) J. Zhang, H. Yu, C. X. Zhang, C. He and C. Y. Duan, *New. J. Chem.,* 2014, **38**, 3137-3145.

9 J. L. Bolliger, A. M. Belenguer and J. R. Nitschke, *Angew. Chem., Int. Ed.*, 2013, **52**, 7958-7962.

10 (a) Q. T. He, X. P. Li, L. F. Chen, L. Zhang, W. Wang and C. Y. Su, *ACS Catal.,* 2013, **3**, 1-9. (b) Y. Huang, Z. Lin and R. Cao, *Chem. Eur. J.,* 2011, **17**, 12706-12712. (c) Y. Huang, T. Ma, P. Huang, D. Wu, Z. Lin and R. Cao, *ChemCatChem*, 2013, **5**, 1877-1883.

11 (a) M. H. Chisholm, *Coord. Chem. Rev.*, 2013, **257**, 1576-1583. (b) F. A. Cotton, C. A. Murillo and R. A. Walton, Multiple Bonds Between Metal Atoms, Springer Science and Business Media, Inc. 2005. (c) F. A. Cotton, C. Lin and C. A. Murillo, *Acc. Chem. Res.,* 2001, **34**, 759-771.

12 M. J. Byrnes, M. H. Chisholm and N. J. Patmore, *Inorg. Chem*., 2005, **44**, 9347-9352.

13 (a) R. P. Bonar-Law, T. D. McGrath, N. Singh, J. F. Bickley and A. Steiner, *Chem. Commun.*, 1999, 2457-2458. (b) R. P. Bonar-Law, J. F. Bickley, C. Femoni and A. Steiner, *J. Chem. Soc., Dalton Trans.,* 2000, 4244-4246.

14 B. Moulton, J. J. Lu, A. Mondal and M. J. Zaworotko, *Chem. Commun.,* 2001, 863-864.

15 (a) M. J. Prakash, Y. Zou, S. Hong, M. Park, M.-P. N. Bui, G. H. Seong and M. S. Lah, *Inorg. Chem.,* 2009, **48**, 1281-1283. (b) M. J. Prakash, M. Oh, X. Liu, K. N. Han, G. H. Seong and M. S. Lah, *Chem. Commun.,* 2010, **46**, 2049-2051.

16 (a) F. A. Cotton, L. M. Daniels, C. Lin and C. A. Murillo, *Chem. Commun.,* 1999, 841-842. (b) F. A. Cotton, C. Lin and C. A. Murillo, *Inorg. Chem*., 2001, **40**, 472-477. (c) F. A. Cotton, C. Lin and C. A. Murillo, *Inorg. Chem.,* 2001, **40**, 478-484. (d) F. A. Cotton, C. Lin and C. A. Murillo, *Inorg. Chem.,* 2001, **40**, 575-577.

17 (a) F. A. Cotton, L. M. Daniels, C. Lin, C. A. Murillo and S. Y. Yu, *J. Chem. Soc., Dalton Trans.*, 2001, 502-504. (b) F. A. Cotton, C. Lin and C. A. Murillo, *Inorg. Chem.,* 2001, **40**, 6413-6417. (c) F. A. Cotton, C. A. Murillo, X. P. Wang and R. M. Yu, *Inorg. Chem.,* 2004, **43**, 8394-8403. (d) F. A. Cotton, C. A. Murillo and R. M. Yu, *Inorg. Chem.,* 2005, **44**, 8211-8215.

18 P. Angaridis, J. F. Berry, F. A. Cotton, C. A. Murillo and X. P. Wang, *J. Am. Chem. Soc.,* 2003, **125**, 10327-10334.

19 (a) M. Eddaoudi, J. Kim, J. B. Wachter, H. K. Chae, M. O'Keeffe and O. M. Yaghi, *J. Am. Chem. Soc.,* 2001, **123**, 4368-4369. (b) Z. Ni, A. Yassar, T. Antoun and O. M. Yaghi, *J. Am. Chem. Soc.,* 2005, **127**, 12752-12753. (c) H. Furukawa, J. Kim, K. E. Plass and O. M. Yaghi, *J. Am. Chem. Soc.,* 2006, **128**, 8398-8399. (d) H. Furukawa, J. Kim, N. W. Ockwig, M. O'Keeffe and O. M. Yaghi, *J. Am. Chem. Soc.,* 2008, **130**, 11650-11661.

20 (a) J. R. Li and H. C. Zhou, *Angew. Chem., Int. Ed.,* 2009, **48**, 8465-8468. (b) J. R. Li, D. J. Timmons and H. C. Zhou, *J. Am. Chem. Soc.,* 2009, **131**, 6368-6369. (c) D. Zhao, D. Q. Yuan, R. Krishna, J. M. van Baten and H. C. Zhou, *Chem. Commun.,* 2010, **46**, 7352-7354. (d) J. R. Li and H. C. Zhou, *Nat. Chem.,* 2010, 2, 893-898. (e) D. Zhao, S. W. Tan, D. Q. Yuan, W. G. Lu, Y. H. Rezenom, H. L. Jiang, L. Q. Wang and H. C. Zhou, *Adv. Mater.,* 2011, **23**, 90-93. (f) T. F. Liu, Y. P. Chen, A. A. Yakovenko and H. C. Zhou, *J. Am. Chem. Soc.,* 2012, **134**, 17358-17361. (g) J. Park, L. B. Sun, Y. P. Chen, Z. Perry and H. C. Zhou, *Angew. Chem., Int. Ed.,* 2014, **53**, 5842-5846. (h) J. Park, Y. P. Chen, Z. Perry, J. R. Li and H. C. Zhou, *J. Am. Chem. Soc.,* 2014, **136**, 16895-16901.

21 (a) Y. X. Ke, D. J. Collins and H. C. Zhou, *Inorg. Chem.,* 2005, **44**, 4154-4156. (b) J. R. Li, A. A. Yakovenko, W. G. Lu, D. J. Timmons, W. J. Zhuang, D. Q. Yuan and H. C. Zhou, *J. Am. Chem. Soc.,* 2010, **132**, 17599-17610.

22 M. D. Young, Q. Zhang and H. C. Zhou, *Inorg. Chem. Acta,* 2015, **424**, 216-220.

23 (a) Y. Zou, M. Park, S. Hong and M. S. Lah, *Chem. Commun.*, 2008, 2340-2342. (b) Z. J. Zhang, W. Shi, Z. Niu, H. H. Li, B. Zhao, P. Cheng, D. Z. Liao and S. P. Yan, *Chem. Commun.,* 2011, **47**, 6425-6427. (c) J. R. Li, J. M. Yu, W. G. Lu, L. B. Sun, J. Sculley, P. B. Balbuena and H. C. Zhou, *Nat. Commun.,* 2013, **4**, 1538-1545.

24 (a) E. Whelan, M. Devereux, M. McCann and V. McKee, *Chem. Commun*., 1997, 427-428. (b) W. G. Lu, D. Q. Yuan, A. Yakovenko and H. C. Zhou, *Chem. Commun.,* 2011, **47**, 4968-4970. (c) L. Chen, J. Kang, H. Cui, Y. Wang, L. Liu, L. Zhang and C.-Y. Su, *Dalton Trans.,* 2015, **44**, 12180-12188. (d) M. Paul, N. N. Adarsh and P. Dastidar, *Cryst. Growth Des.,* 2014, **14**, 1331-1337 (e) F. A. Cotton, C. A. Murillo, S. E. Stiriba, X. P. Wang and R. M. Yu, *Inorg. Chem.*, 2005, **44**, 8223-8233.

25 (a) P. Muller and C. Fruit, *Chem. Rev.,* 2003, **103**, 2905-2919. (b) G. Dequirez, V. Pons and P. Dauban, *Angew. Chem., Int. Ed.,* 2012, **51**, 7384-7395. (c) J. L. Roizen, M. E. Harvey and J. Du Bois, *Acc. Chem. Res.,* 2012, **45**, 911-922.

26 (a) B. J. Stokes, H. J. Dong, B. E. Leslie, A. L. Pumphrey and T. G. Driver, *J. Am. Chem. Soc.,* 2007, **129**, 7500-7501. (b) H. Dong, M. Shen, J. E. Redford, B. J. Stokes, A. L. Pumphrey and T. G. Driver, *Org. Lett*., 2007, **9**, 5191-5194. (c) M. H. Shen, B. E. Leslie and T. G. Driver, *Angew. Chem., Int. Ed.,* 2008, **47**, 5056-5059. (d) B. J. Stokes, B. Jovanovic, H. J. Dong, K. J. Richert, R. D. Riell and T. G. Driver, *J. Org. Chem.,* 2009, **74**, 3225-3228. (e) K. Sun, S. Liu, P. M. Bec and T. G. Driver, *Angew. Chem., Int. Ed.,* 2011, **50**, 1702-1706. (f) B. J. Stokes, S. Liu and T. G. Driver, *J. Am. Chem. Soc.,* 2011, **133**, 4702-4705. (g) A. L. Pumphrey, H. J. Dong and T. G. Driver, *Angew. Chem., Int. Ed.,* 2012, **51**, 5920-5923. (h) Q. Nguyen, K. Sun and T. G. Driver, *J. Am. Chem. Soc.,* 2012, **134**, 7262-7265. (i) C. Kong, N. Jana and T. G. Driver, *Org. Lett.,* 2013, **15**, 824-827. (j) C. Jones, Q. Nguyen and T. G. Driver, *Angew. Chem., Int. Ed.,* 2014, **53**, 785-788. (k) C. Jones, D. Boudinet, Y. Xia, M. Denti, A. Das, A. Facchetti and T. G. Driver, *Chem. Eur. J.,* 2014, **20**, 5938-5945. (l) B. J. Stokes, K. J. Richert and T. G. Driver, *J. Org. Chem.,* 2009, **74**, 6442-6451.

27 W. G. Shou, J. Li, T. Guo, Z. Lin and G. Jia, *Organometallics,* 2009, **28**, 6847-6854.

28 O. V. Dolomanov, L. J. Bourhis, R. J. Gildea, J. A. K. Howard and H. Puschmann, *J. Appl. Cryst*., 2009, **42**, 339-341.

29 G. M. Sheldrick, SHELX 97, Program for Crystal Structure Solution and Refinement, Göttingen University, 1997

30 G. M. Sheldrick, *Acta Cryst.,* 2008, A64, 112-122.

View Article Online
DOI: 10.1039/C5TA05592J

31 (a) Taber, D. F.; Meagley, R. P.; Louey, J. P.; Rheingold, A. L. *Inorg. Chem. Acta,* 1995, 239, 25-28. (b) H. M. L. Davies and C. Venkataramani, *Org. Lett.,* 2003, **5**, 1403-1406. (c) C. G. Espino, K. W. Fiori, M. Kim and J. Du Bois, *J. Am. Chem. Soc.,* 2004, **126**, 15378-15379. (d) J. Du Bois, *Chemtracts-Org. Chem.,* 2005, **18**, 1-13. (e) D. N. Zalatan and J. Du Bois, *J. Am. Chem. Soc.,* 2009, **131**, 7558-7559.

32 A. L. Spek, *J. Appl. Crystallogr,* 2003, **36**, 7-13.

33 (a) S. A. Johnson, H. R. Hunt and H. M. Neumann, *Inorg. Chem.,* 1963, **2**, 960-962. (b) D. C. Wynne, M. M. Olmstead and P. G. Jessop, *J. Am. Chem. Soc.,* 2000, **122**, 7638-7647.

34 a) K. Tan, N. Nijem, P. Canepa, Q. Gong, J. Li, T. Thonhauser and Y. J. Chabal, *Chem. Mater.,* 2012, **24**, 3153-3167. (b) A. Doyle, J. Felcman, M. T. D. Gambardella, C. N. Verani and M. L. B. Tristão, *Polyhedron*, 2000, **19**, 2621-2627.

35 F. A. Cotton, E. A. Hillard and C. A. Murillo, *J. Am. Chem. Soc*., 2002, **124**, 5658-5660.

36 (a) K. M. Kadish, D. Lancon, A. M. Dennis and J. L. Bear, *Inorg. Chem*., 1982, **21**, 2987-2992. (b) A. M. Dennis, J. D. Korp, I. Bernal, R. A. Howard and J. L. Bear, *Inorg. Chem*., 1983, **22**, 1522-1529. (c) T. P. Zhu, M. Q. Ahsan, T. Malinski, K. M. Kadish and J. L. Bear, *Inorg. Chem*., 1984, **23**, 2-3.

37 (a) M. Q. Ahsan, I. Bernal and J. L. Bear, *Inorg. Chem*., 1986, **25**, 260-265. (b) J. F. Múnera, S. Irusta, L. M. Cornaglia, E. A. Lombardo, D. V. Cesar and M. Schmal, *J. Catal.,* 2007, **245**, 25-34. (c) V. Abdelsayed, D. Shekhawat, J. A. Poston and J. Spivey, *J. Catal. Today*, 2013, **207**, 65-73.